

Original Research

A Novel Signature Composed of Hypoxia, Glycolysis, Lactylation Related Genes to Predict Prognosis and Immunotherapy in Hepatocellular Carcinoma

Feng Yi¹, Shichao Long^{1,2}, Yuanbing Yao¹, Kai Fu^{1,3,4,5},*

Academic Editor: Jordi Sastre-Serra

Submitted: 30 November 2024 Revised: 17 March 2025 Accepted: 21 March 2025 Published: 21 April 2025

Abstract

Background: Hepatocellular carcinoma (HCC) is one of the leading causes of cancer death worldwide. The hypoxic microenvironment in HCC enhances glycolysis and co-directed lactate accumulation, which leads to increased lactylation. However, the exact biological pattern remains to be elucidated. Therefore, we sought to identify hypoxia-glycolysis-lactylation (HGL) prognosis-related signatures and validate this in vitro. Methods: Transcriptomic data of patients with HCC were collected from The Cancer Genome Atlas (TCGA), International Cancer Genome Consortium (ICGC), and Gene Expression Omnibus (GEO) databases. Differentially expressed HGL genes between HCC and normal tissues were obtained by DEseq2. The consensus clustering algorithm was employed to stratify patients into two distinct clusters. Subsequently, the single sample Gene Set Enrichment Analysis (ssGSEA), Tumor Immune Estimation Resource (TIMER) and Tumor Immune Dysfunction and Exclusion (TIDE) algorithms were utilized to assess immune infiltration and immune evasion. Least Absolute Shrinkage and Selection Operator (LASSO) and COX regression analysis were used to identify an HGL prognosis-related signature. Based on spatial transcriptome and histological data, we analyzed the expression of these genes in HCC and explored the function of Homer Scaffold Protein 1 (HOMER1) in HCC cells. Results: We identified 72 differentially expressed HGL genes and two HGL clusters. Cluster2, with better survival (p < 0.001), was significantly enriched in metabolic-related pathways. The HGL prognosis-related signature exhibited great predictive efficacy for patients in TCGA, ICGC, and GSE148355 databases (3-year area under the curve (AUC) = 0.822, 0.738, and 0.707, respectively). The elevated expression of HOMER1 in HCC was revealed by the combination of spatial transcriptome and histological data. Knocking down HOMER1 significantly inhibited the malignant progression of HCC cells. Conclusions: We identified a signature with great predictive efficacy and discovered a gene, HOMER1, that influences the malignant progression of HCC with the potential to become a novel therapeutic target.

Keywords: hepatocellular carcinoma; lactylation; hypoxia; glycolysis; HOMER1

1. Introduction

Hepatocellular carcinoma (HCC) is the major histologic subtype of liver cancer, the third most common cause of cancer-related mortality worldwide [1]. At present, surgical treatment along with ablation, radiotherapy, chemotherapy, immunotherapy and targeted therapy, constitute the main form of treatment [2]. Accurate and effective classification can help to select the most suitable treatment for patients with HCC [3]. Along with the rapid development of multi-omics, the molecular characteristics along with immune and metabolic microenvironment helps to measure precise and effective treatments for patients with HCC [4,5]. However, the independent prognostic factors for HCC are still limited.

Metabolic reprogramming is one of the hallmark features of tumors. In the process of continuous proliferation [6], invasion and metastasis, the microenvironment gradually becomes nutrient-deficient. In order to cope with the nutrient-deficient microenvironment, the tumor constantly changes its metabolic characteristics to adapt. HCC is characterized by a variety of metabolic changes: first, changes in energy metabolism occur. The hypoxic environment and tumor characteristics lead to enhanced glycolysis and lactate accumulation; increased fatty acid synthesis supports the production of cell membranes and energy storage. Amino acid metabolism is also altered, resulting in an increasing in glutamine, which plays a role in cellular energy metabolism and antioxidant responses [7].

¹Institute of Molecular Precision Medicine and Hunan Key Laboratory of Molecular Precision Medicine, Department of General Surgery, Xiangya Hospital, Central South University, 410083 Changsha, Hunan, China

²Department of Radiology, and National Clinical Research Center for Geriatric Disorders, Xiangya Hospital, Central South University, 410083 Changsha, Hunan, China

³Center for Medical Genetics & Hunan Key Laboratory of Medical Genetics, School of Life Sciences, Central South University, 410083 Changsha, Hunan, China

⁴National Clinical Research Center for Geriatric Disorders, 410114 Changsha, Hunan, China

⁵Hunan Key Laboratory of Aging Biology, Xiangya Hospital, Central South University, 410083 Changsha, Hunan, China

^{*}Correspondence: fu kai@csu.edu.cn (Kai Fu)

Hypoxia is one of the common features of malignant solid tumors [8], which also promotes the malignant process of HCC. The malignant proliferation of HCC will consume an increased supply of oxygen and create a hypoxic tumor microenvironment. Hypoxia can activate the Hypoxia-Inducible Factor (HIF) signaling pathway, which is a core transcription factor in the hypoxic response. HIF sense low oxygen levels and regulate the expression of various genes, promoting the survival and proliferation of tumor cells in the hypoxic environment [9]. Hypoxia also plays a crucial role in the development of chemoradiotherapy resistance and immune evasion [9–12]. As a major form of glucose metabolism, glycolysis is the primary energy source for tumor cells. It is also key in driving malignant proliferation, invasion, metastasis, and drug resistance in HCC [7,10–13]. These processes interact with each other and collectively play an important role in the progression of HCC.

Hypoxia promotes glycolysis which produces lactate, which is the substrate for lactylation. It is a new form of protein post-transcriptional modification, which regulates the proteins by covalently coupling lactyl to lysine residues. The lactylation of histones can affect the binding ability of histones to DNA and alter the structure and function of chromatin. In the past two years, a growing body of research has begun to reveal the link between lactylation and tumor progression. It plays an important role in regulating DNA damage repair pathways, thus affecting the formation of chemoradiotherapy resistance [14,15]. It also has been reported that lactylation can promote the proliferation and metastasis of HCC [16]. Employing hypoxia, glycolysis, or lactylation genesets alone to predict survival in hepatocellular carcinoma has been reported [12,17,18]. However, considering the relevance of three metabolic processes, it is worth exploring whether combining genesets could make more accurate predictions for HCC patients.

HOMER1 (also known as Homer Scaffold Protein 1) is a protein that is mainly expressed in the nervous system [19] and belongs to the Homer protein family. HOMER1 regulates a variety of signaling pathways in cells, including calcium signaling, G protein-coupled receptor signaling, and N-Methyl-D-Aspartate receptor function, mainly by interacting with other proteins. Recent studies have found that HOMER1 not only plays an important role in the nervous system, but also is closely related to the occurrence and development of tumors [20,21]. HOMER1 has also been reported to be associated with HCC tumorigenesis and maybe a potential therapeutic target for HCC.

In this study, we divided HCC patients into two clusters based on the hypoxia-glycolysis-lactylation (HGL) gene set. Based on the two clusters of differentially expressed genes, we identified a signature with great predictive power and also found a malignant target gene, HOMER1. We have verified that the expression of HOMER1 is elevated in HCC by a combination of spatial transcriptome and histological data. Cell assays have revealed that it can affect the malignant progression of HCC.

2. Materials and Methods

2.1 Acquisition of Transcriptome and Spatial Transcriptome Data

Transcriptomic data and clinical information of HCC patients were obtained from TCGA-LIHC (The Cancer Genome Atlas database-Liver Hepatocellular Carcinoma, n = 370; https://www.cancer.gov/ccg/research/genome-seq uencing/tcga), the International Cancer Genome Consortium (ICGC-LIHC, n = 232), which were downloaded from UCSC XENA (https://xenabrowser.net/). GSE148355 (n = 52) was derived from the Gene Expression Omnibus (GEO) database (https://www.ncbi.nlm.nih.gov/geo/). Hypoxia and glycolysis-related gene sets were obtained from the Molecular Signature Database (GSEA | MSigDB (https: //gsea-msigdb.org)), and lactylation-related gene sets were obtained from a previously published study [17]. To investigate the spatial expression of each gene in the signature, spatial transcriptomic data was downloaded from a previous study [22] (https://ngdc.cncb.ac.cn/gsa-human/browse/ HRA000437), and subsequent analysis was performed using the 'Seurat' R package (https://cran.r-project.org/web/p ackages/Seurat/index.html, v5.1.0).

2.2 Differential HGL Genesets

The hypoxia, glycolysis and lactylation genesets were derived from a previously published study [17] and the Molecular Signature Database (GSEA | MSigDB (https://gsea-msigdb.org)). We obtained the differentially expressed genes (DEGs) in HCC patients versus normal individuals with the 'DEseq2' R package (https://github.com/thelovelab/DESeq2, v1.38.3), by the criteria of FDR <0.05 and $|\log 2fc| \ge 1$.

2.3 Enrichment Analysis and Consensus Clustering Analysis

Employing univariate COX analysis, prognostic HGL genes were obtained, then Kyoto Encyclopedia of Genes and Genomes (KEGG, https://www.genome.jp/kegg/), Gene Ontology (GO, https://www.geneontology.org/), Gene Set Enrichment Analysis (GSEA, https://www.gsea-msigdb.org/gsea/index.jsp) enrichment analysis were performed.

The TCGA-LIHC patients were divided into two clusters with prognostic HGL genes using the 'CancerSubtypes' R package (https://github.com/taoshengxu/CancerSubtypes, v.1.24.0).

2.4 Assessment of Immune Infiltration and Immune Evasion

To compare the immune microenvironment between the two clusters, we predicted differences in infiltration of 6 immune cells using the Tumor Immune Estimation Resource (TIMER) algorithm (http://cistrome.org/TIMER/). The difference of immune function was predicted by the 'GSVA' R package (https://github.com/rcastelo/GSVA,



v1.46.0) [23]. The immune evasion ability of the two clusters was evaluated by the Tumor Immune Dysfunction and Exclusion (TIDE) algorithm (http://tide.dfci.harvard.edu/).

2.5 Prediction of Drug Sensitivity

To assess the guiding potential of HGL clustering for clinical drug use, we measured the 'PRROPHETIC' R package (https://github.com/paulgeeleher/pRRophetic, v0.5) to predict IC50 values for each drug and compared differences between the two clusters for commonly used drugs in HCC.

2.6 Establishment and Validation of HGL Signature

We obtained DEGs between 2 clusters with the 'Limma' R package (https://www.bioconductor.org/packages/release/bioc/html/limma.html, v3.54.2), the criteria were $|\log 2\text{fc}| \ge 1$, p < 0.05; then measured COX LASSO regression screening for genes to construct the optimal model. The 'Survminer' R package (https://cran.r-project.org/web/packages/survminer/index.html, v0.5.0) was used for Kaplan-Meier (K-M) survival analysis to compare the difference of Overall Survival (OS) between high-risk and low-risk groups in different data sets. The predictive ability of this signature was further evaluated using 'time-ROC' R package (https://cran.r-project.org/web/packages/timeROC/, v0.4.0) to calculate the receiver operating characteristic (ROC) curve and the area under the curve (AUC).

We explored the association between the HGL signature (HGLs) and clinical features, finding that HGLs had an independent ability to predict patients' outcomes by K-M analysis.

2.7 Tissue Acquisition of HCC Patients

A total of 8 pairs of HCC adjacent and tumor tissues were obtained from the Xiangya Hospital, Central South University. The Central South University Xiangya Hospital Ethics Committee approved this study. All patients or their families/legal guardians obtained their informed consent to use their materials. The patient's clinical information is presented in **Supplementary Table 1**.

2.8 Real Time Quantitative PCR (RT-qPCR) and Western Blotting

The tissue samples from patients were cryogenically ground, followed by RNA extraction using the TRIZOL reagent (ET101-01-V2, Transcript®, Beijing, China). The extracted RNA was then reverse transcribed into cDNA using the reverse transcription kit (E047-01B, NovoScript®, Suzhou, China). Finally, the PCR reaction system mixed with primers and cDNA was prepared. Primers used are listed in **Supplementary Table 2**. To calculate the relative expression of HOMER1, we used β -actin as a reference gene, the $2^{-\Delta\Delta Ct}$ method is used: $\Delta Ct = Ct_{HOMER1} - Ct_{\beta-actin}, \Delta\Delta Ct = \Delta Ct_{Tumor} - \Delta Ct_{Normal}$, Relative Expression = $2^{-\Delta\Delta Ct}$.

Tissue or cell lysates were prepared using lysis buffer and protein concentrations were measured. The protein was separated by SDS-PAGE and transferred to a nitrocellulose membrane. The membrane was blocked with 5% milk, followed by incubation with the primary antibody overnight at 4 °C. After washing with Tris-Borate-Sodium Tween-20 (TBST) buffer, the membrane was incubated with the secondary antibody for 2 hours. Protein was visualized using chemiluminescent detection. Antibodies used were as follows: HOMER1 (1:1000, db12743, Diagbio, Hangzhou, China), β -Tubulin (1:10,000, 66240-1-Ig, Proteintech, Wuhan, China), Peroxidase-conjugated AffiniPure Goat Anti-Mouse IgG (H+L) (1:5000, 115-035-003, Jackson, West Grove, PA, USA), Peroxidase-conjugated AffiniPure Goat Anti-Rabbit IgG (H+L) (1:5000, 111-035-003, Jackson, West Grove, PA, USA).

2.9 Cell Culture and Transfection

LM3 and Hep3B in this study were purchased from BDBIO (Zhejiang, China). The two types of cells have been successfully authenticated by STR profiling and have passed mycoplasma testing. They were cultured in DMEM medium (10% FBS) under 5% $\rm CO_2$ at 37 °C.

According to the knocking down of HOMER1, Hep3B and LM3 cell lines were transfected with lipofectamine 2000 following the manufacturer's instructions. All small interfering RNA (siRNA) fragments were designed and synthesized by Gene Pharma (Shanghai, China); and are listed in **Supplementary Table 3**.

2.10 Flow Cytometry Measures the Cell Cycle

After knocking down HOMER1 in Hep3B and LM3 cells as mentioned above, they were incubated for 72 hours. Then the cells were digested and collected in a cell suspension, and washed with PBS. The cells were fixed by incubating with 70% ethanol for 12 hours. After removing the ethanol, the cells were permeabilized using 0.1% Nonidet P-40 (NP-40) (N8030, Solarbio®, Beijing, China). Finally, the cells were stained with propidium iodide for 30 minutes (The propidium iodide solution is prepared by combining 3 mL of staining buffer, 150 μ L of 20× propidium iodide staining solution, and 60 μ L of 50× RNase A), and analyzed at different cell cycle stages using flow cytometry based on the fluorescence intensity.

2.11 Wound Healing Assay

Hep3B and LM3 cells were seeded in 6 cm dishes, and transfected with a mixture of 2 μ L of lipofectamine 2000, 200 μ L of Opti-MEM, and 3 μ L of siHOMER1 to knock down the expression of HOMER1 in both cell lines; subsequently 1 \times 10⁵ cells were seeded into each six-well plate; scratches were made with 10 μ L pipette until cells were 100% the following day. The images were taken at 0 h and 24 h. The statistical results were analyzed by ImageJ (V1.54g, National Institutes of Health, Bethesda, MD, USA).



2.12 Colony Formation Assay

After transfected with HOMER1 siRNA or random control, 500 cells were seeded into six-well plates, and 10 days later fixed with 4% paraformaldehyde (G1101, Servicebio, Wuhan, China) and stained with crystal violet solution. The statistical results were analyzed by ImageJ.

2.13 Transwell Assay

We used a 24-hole Transwell chamber (Transwell, Corning Costar, Corning, NY, USA). For migration assays, 2×10^4 cells were seeded in the upper chamber, cultured in serum-free DMEM, and 20% serum DMEM was added in the lower chamber. For the invasion assay, 30 μL Matrigel was used to coat the superior compartment, and then 2×10^5 cells were seeded into the superior compartment. After 48 hours of culture, the cells were fixed with 4% paraformaldehyde, stained with crystal violet, then swabbed to remove the upper cells. The statistical results were analyzed by ImageJ.

3. Results

3.1 Expression and Pathway Enrichment of HGL Genesets in HCC

We obtained 149 HGL-DEGs between tumor and normal tissues (Fig. 1A,B). Univariate COX regression showed that 72 genes were significantly associated with the prognosis of HCC. The GO and KEGG enrichment analyses revealed that prognostic-associated HGL genes were associated with metabolism-related pathways, including glycolysis, the HIF-1 signaling pathway, and organic acid catabolic and carboxylic acid catabolic processes (Fig. 1C,D). It reveals that both hypoxia, glycolysis and lactylation effect the prognosis of HCC.

3.2 Construction of HGL Clusters and TME Signatures of HGL Clusters

Based on the prognostic-associated HGL genes, we conducted a consensus clustering algorithm on the TCGA-LIHC dataset to further investigate the effect of HGL on HCC. When K=2, we obtained the appropriate clustering result (Fig. 2A). Principal component analysis (PCA) also displayed that the two clusters were separated visibly (Fig. 2B). K-M curves revealed that patients in cluster1 had better median survival time than those in cluster2 (Fig. 2C, p < 0.001). GSEA analysis revealed that pathways enriched in cluster1 were mainly metabolic-related pathways, while cluster2's were related to the malignant process of HCC. These pathways include: E2F_TARGETS, G2M_CHECKPOINT, EPITHE-LIA_MESENCHYMAL_TRANSITION (Supplementary Fig. 1A,B).

There were variances in immune cells between the two clusters (Fig. 2D). The check-point function of cluster2 was significantly higher than that of cluster1 (Fig. 2E, p < 0.05).

PDCD1, CLTLA4, LAG3, and Haver2, the major inhibitory immune checkpoint receptors in HCC [24], were highly expressed in cluster2 (Fig. 2F, p < 0.001). A TIDE score of cluster2 was also higher than that of cluster1 (Fig. 2G, p < 0.01), which suggests that cluster1 may have a better response to immunotherapy.

3.3 Drug Sensitivity Prediction

Chemotherapy and immunotherapy are both important therapeutic methods for HCC. After IC50 prediction of chemotherapeutic drugs, we found that patients in cluster1 were more sensitive to sorafenib than patients in cluster2 (p < 0.001). The same is true for other drugs, such as: 5-Fluorouracil, etoposide, cytarabine, docetaxel, cisplatin, doxorubicin, nilotinib, paclitaxel, gemcitabine, gefitinib, sunitinib, vinblastine (p < 0.001). Overall, the drug sensitivity of cluster1 was superior to cluster2 (Fig. 3).

3.4 Construction and Validation of HGL Prognosis-Related Signature

We performed differential analysis between the two clusters, and after conducting univariate COX regression analysis on the differentially expressed genes, we finally identified these 123 survival-related differential genes (Fig. 4A). Using LASSO and multivariate COX regression, we acquired 13 genes to construct the signature (Supplementary Fig. 2A). The riskScore calculation was as follows: riskScore = $(0.20233 \times CDCA8) + (0.140306 \times GAGE2D) + (0.0913041 \times S100A9) + (-0.08057605 \times SLC16A11) + (-0.1422534 \times SOCS2) + (0.0711202 \times FAM163A) + (-0.08746885 \times LGSN) + (0.09041832 \times FRMD1) + (0.09532562 \times HOMER1) + (-0.1636347 \times CD8B) + (-0.1596561 \times CD27) + (0.1255294 \times E2F5) + (01694574 \times PGF).$

The patients in the TCGA training set were divided into a high-risk group (N = 185) and low-risk group (N = 185) based on the riskScore, while the OS of the low-risk group was significantly better than the high-risk group (Fig. 4B, p < 0.001). The risk curve also showed that as the risk score increases, the survival rate decreases (Fig. 4C). At 1–5 years, the AUC of the ROC curve for risk signature was 0.818, 0.824, 0822, 0.829, and 0.821, respectively, which indicates a great predictive accuracy for HCC patients (Fig. 4D).

To further validate the predictive effectiveness of the signature, we grouped the ICGC and the GSE148355 together, since the validation set was similar: ICGC highrisk group (N = 105), ICGC low-risk group (N = 127), and GSE148355 high-risk group (N = 27), low-risk group (N = 25). Patients in the low-risk group still had significantly better OS than those in the high-risk group (Fig. 4E,F, p < 0.001/p = 0.01). At 1–4 years, the AUC of the ROC curve for ICGC-LIHC were 0.700, 0.720, 0.738, 0.750 (**Supplementary Fig. 2B**), respectively; the AUC for GSE148355 were 0.758, 0.689, 0.707, 0.710



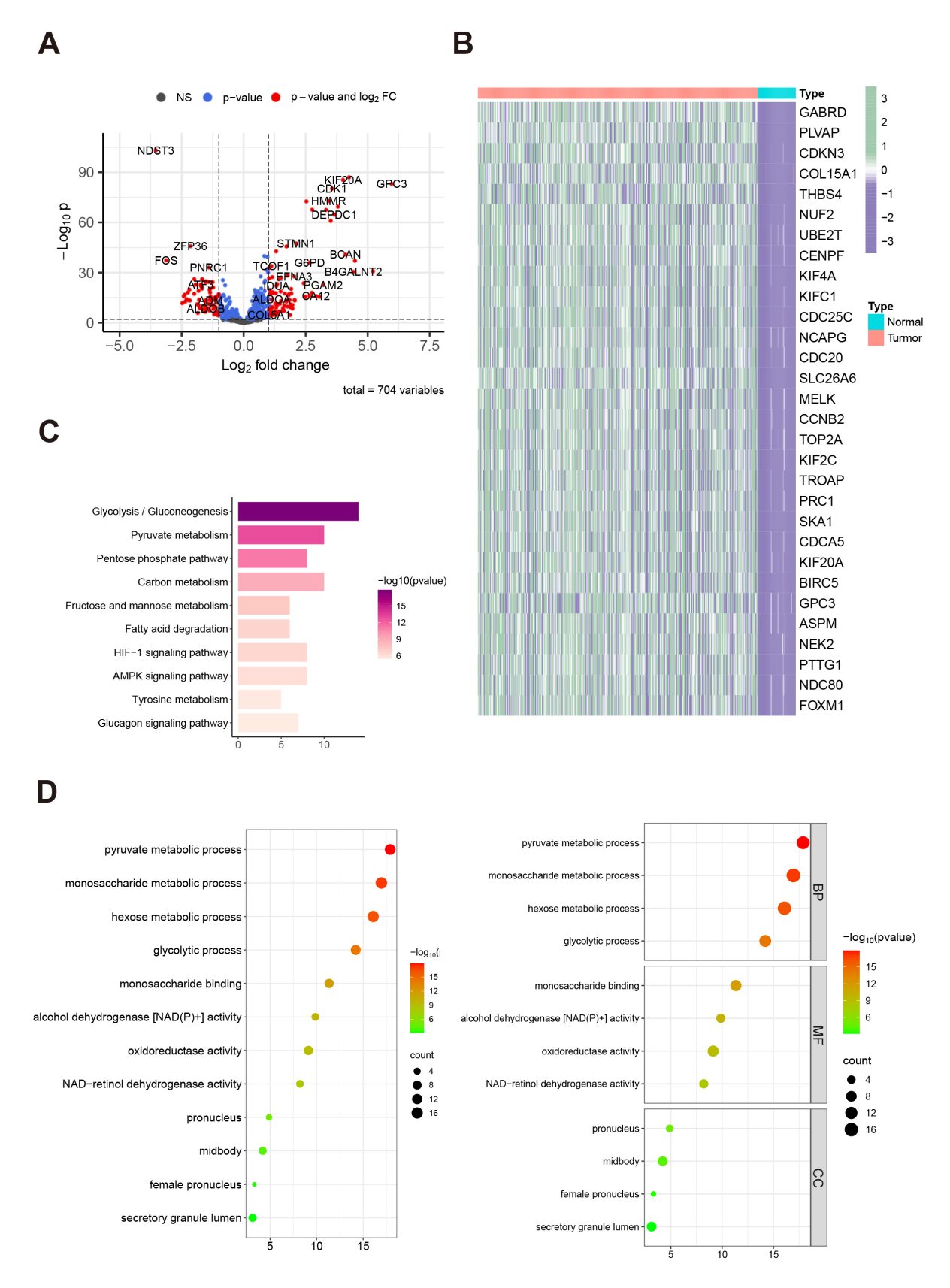


Fig. 1. HGL associate genes differentially expressed in TCGA-LIHC. (A) The volcano plot showing the HGL-DEGs between tumor and normal samples in TCGA dataset. (B) Heatmap showing top 30 DEGs. (C) The bar plot of KEGG enrichment pathway of prognostic-associated HGL genes. (D) GO enrichment analysis bubble plot. HGL, hypoxia-glycolysis-lactylation; TCGA-LIHC, The Cancer Genome Atlas database-Liver Hepatocellular Carcinoma; DEGs, differentially expressed genes; KEGG, Kyoto Encyclopedia of Genes and Genomes; GO, Gene Ontology; NS, no significance.

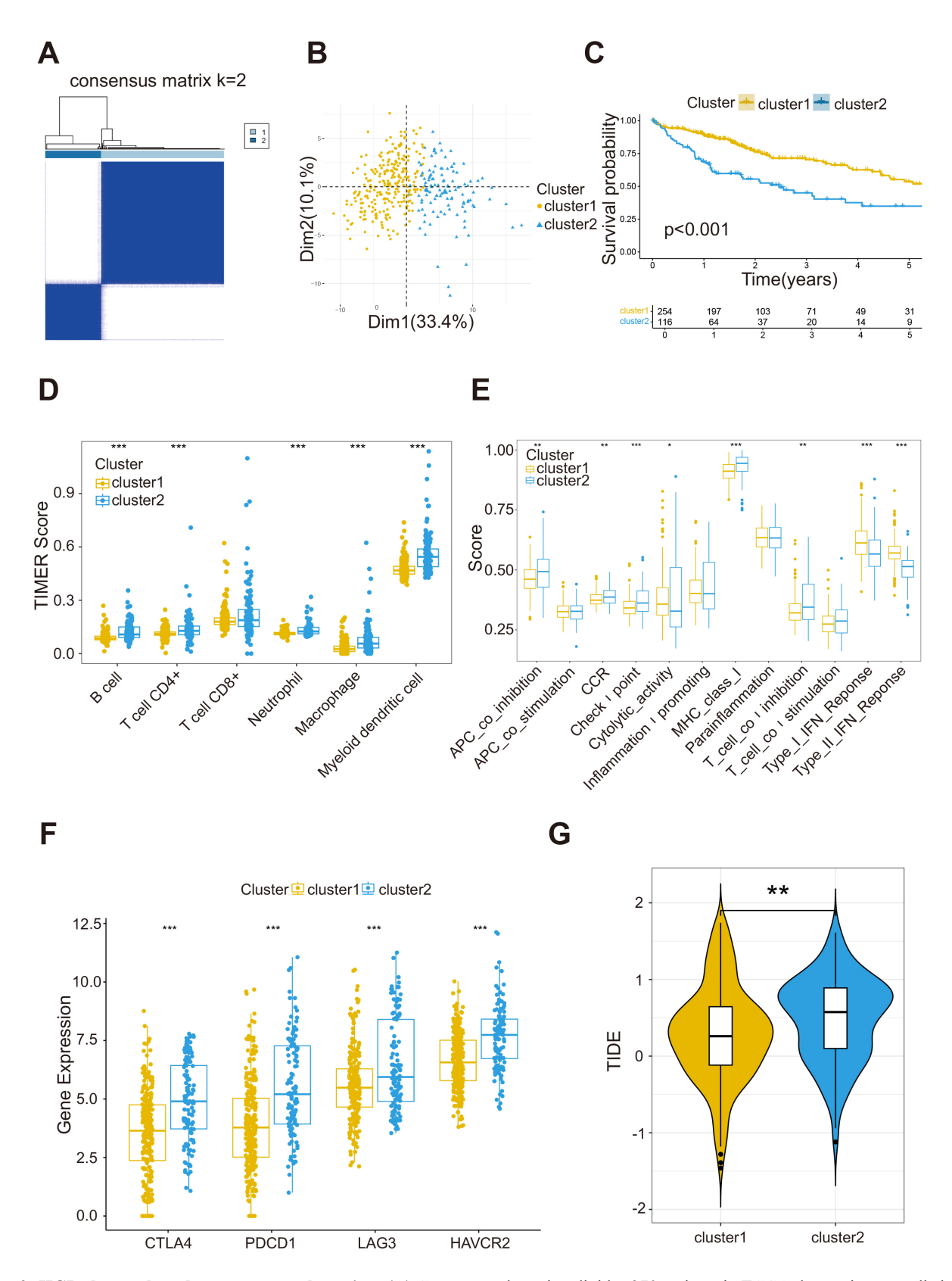


Fig. 2. HGL clusters based on consensus clustering. (A) Consensus clustering divides 370 patients in TCGA dataset into two distinct clusters. (B) PCA analysis shows that the two clusters of patients are significantly segmented. (C) Kaplan-Meier (K-M) curve analysis of cluster1 and cluster2. (D) Infiltration differences of six immune cells between cluster1 and cluster2. (E) The levels of immune function of the two HGL clusters. (F) The immune checkpoint receptor genes are highly expressed in cluster2. (G) Cluster2 has higher TIDE score. Statistical significance was denoted as follows. *p < 0.05, **p < 0.01, ***p < 0.001. PCA, principal component analysis; TIDE, Tumor Immune Dysfunction and Exclusion.

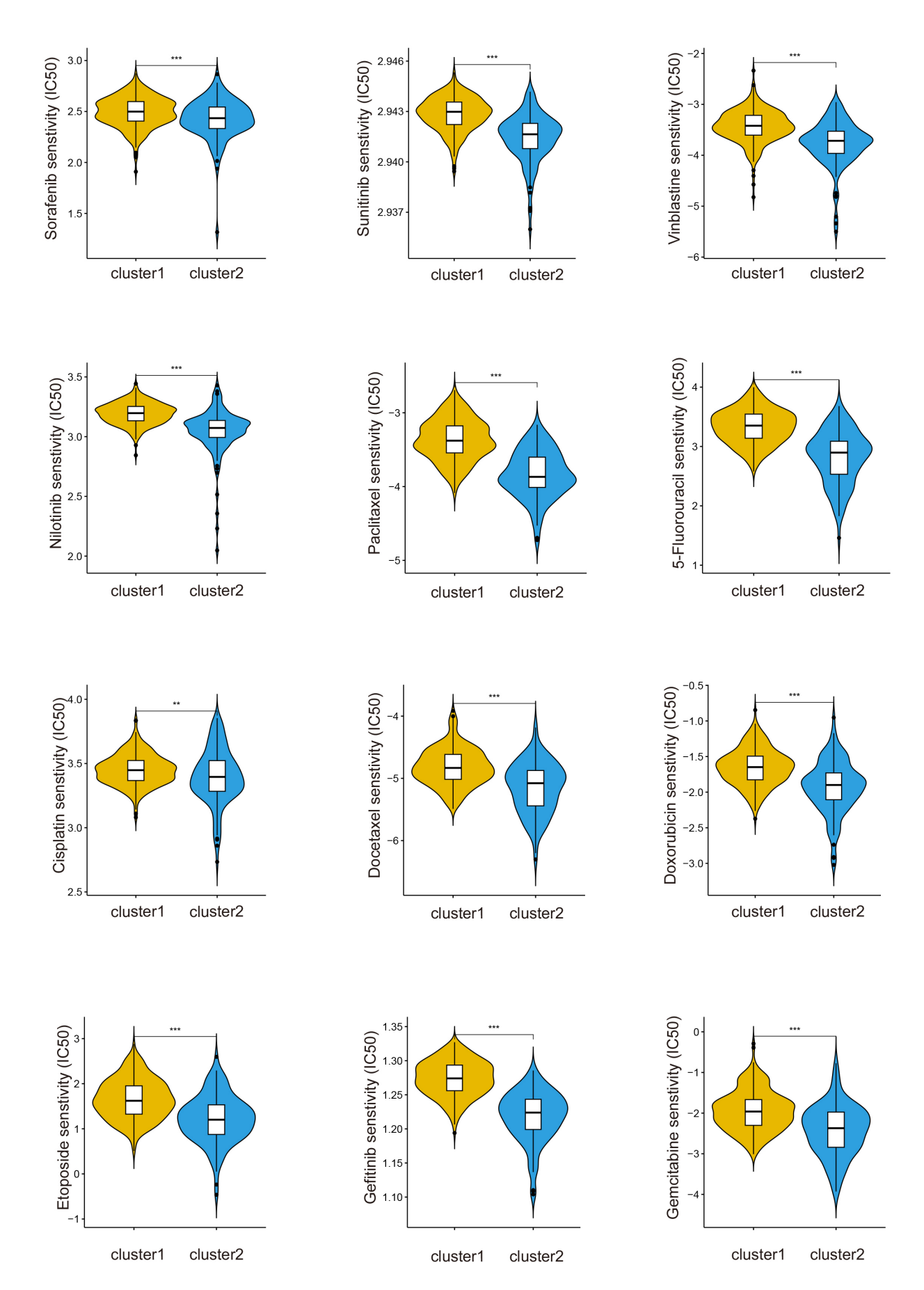


Fig. 3. The drug sensitivity of cluster1 is better than cluster2. **p < 0.01, ***p < 0.001.

(Supplementary Fig. 2C), respectively. The signature also exhibited good prediction ability for these external validation cohorts.

3.5 HGL RiskScore is an Independent Predictor of HCC

HGL signature exhibits predictive power, thus we desired to explore whether it can be used as an independent prognostic factor for HCC patients. Age, gender, alphafetoprotein level (AFP), microvascular invasion (MVI), and pathological stage were crucial factors affecting the prognosis of HCC patients, riskScore could also accurately predict the prognosis. In the K-M curve, patients in different ages, different sex, and in different pathological stages, with different expression of AFP, whether with microvascular invasion or not, showed a significant variance in OS between the high and low risk group (Fig. 5A, p < 0.01). Univariate and multivariate COX analysis showed that the riskScore and pathologic stages were related with the OS of patients according to the univariate COX analysis (Fig. 5B); while the multivariate COX analysis revealed they are also the independent predictors (Fig. 5C).

3.6 Construction and Validation of Nomogram

To obtain a better prediction of prognosis, we incorporated the above clinical factors together with the riskScore to construct a nomogram. Patients with a higher score represent worse survival (Fig. 6A, p < 0.001). The C-index of each factor suggests that the riskScore still contributes the most to the nomogram (Fig. 6B). The survival ROC analysis shows that the AUC were 0.822, 0.676 for riskScore and pathologic stage, which were superior to other clinical factors. The prognostic ability of gender and age is relatively poor, and there are also fewer patients with MVI data in the TCGA-LIHC cohort. As a result, the AUC of these clinical prognostic factors is not ideal (Fig. 6C). The calibration curve revealed that the predicted OS and observed OS have great consistency, and that nomogram has good predictive ability (Fig. 6D).

3.7 The Spatial Transcriptome Data Revealed HOMER1 was Concentrated on HCC

To explore the expression patterns in HCC, we incorporated a set of spatial transcriptomic data to investigate genes in HGL signature from both the expression level and spatial orientation [22]. The organization of four sets of spatial transcriptomes were taken from the junction of tumor and normal tissue, and cells obtained from these samples were divided into 14 cell clusters (Fig. 7A). Based on the annotations that come with the spatial transcriptome data, these cells could be defined as five kinds of localized cell populations, namely: Hepatocytes, Immune infiltration region (IIR), Transition, Tumor, Others (Fig. 7B).

As shown in the bubble diagram, among the genes in the signature, HOMER1 is mainly expressed in tumorderived cells (Fig. 7C). To further validate our findings, we performed spatial transcriptomic analysis on these four sets of samples. From the spatial distribution of the cell clusters and the spatial distribution of HOMER1, we found that HOMER1 highly coincides with the distribution of tumor cells (Fig. 7D,E). The differential expression of HOMER1 indicates that this protein may play a key role in the malignant process of hepatocellular carcinoma.

3.8 HOMER1 is Elevated in HCC Patients and Affects the Proliferation, Invasion and Metastasis of Hepatocellular Carcinoma Cell Lines

The mechanism of HOMER1 in HCC has not been explored, thus we sought to explore the actual expression of HOMER1 in HCC. Eight pairs of adjacent and tumor tissues from HCC patients were obtained. Western blot revealed HOMER1 was elevated in tumor tissues (Fig. 8A,B, p < 0.01); RT-qPCR also confirmed its presence at the transcription level (**Supplementary Fig. 2D**).

To explore its function in hepatocellular carcinoma cell lines, we knocked down HOMER1 in LM3 as well as in Hep3B cell lines, with Western-Blot demonstrating that HOMER1 knock down was very successful (Fig. 8C; Supplementary Fig. 2E,F). We observed that knocking down HOMER1 significantly inhibited the proliferation of LM3 and Hep3B. The colony formation assay clearly exhibited the difference of cell proliferation between untreated and si-HOMER1 cells (Fig. 8D, p < 0.0001). Cell cycle analysis further revealed that knocking down HOMER1 increased the proportion of cells arrested in the G2/M phase (Fig. 8E). These results suggested that HOMER1 may play an important role in the cell cycle of hepatocellular carcinoma cell lines. The wound healing assay showed that HOMER1 knock down also inhibited the migration of LM3 and Hep3B cells (Fig. 9A, p < 0.01), while the Transwell assay confirmed both migration and invasion of LM3 and Hep3B cells were decreased after knocking down of HOMER1 (Fig. 9B,C, p < 0.01). These experiments revealed knocking down HOMER1 could inhibit the proliferation of hepatocellular carcinoma cell lines by blocking the cell cycle, and also affect the invasion and metastasis of hepatocellular carcinoma cell lines.

4. Discussion

The lactylation of histones is a new method for protein modification. In the past two years, it has been reported that lactylation has a definite regulatory effect on tumor progression, chemoradiotherapy resistance, and immune evasion. Lactylation has also been reported in hepatocellular carcinoma: Lactylation at K28 inhibits the function of Adenylate kinase and promotes the proliferation and metastasis of hepatocellular carcinoma cell; while the lactylation of Aldolase A (ALDOA) at the K230/322 site can affect its binding to DEAD-box helicase 17 (DDX17), thus regulating the stemness of hepatocytes.

Lactylation is vital to tumor progression. There have been numerous studies on constructing prognosis signature based on lactylation genesets: Huang *et al.* [25] de-



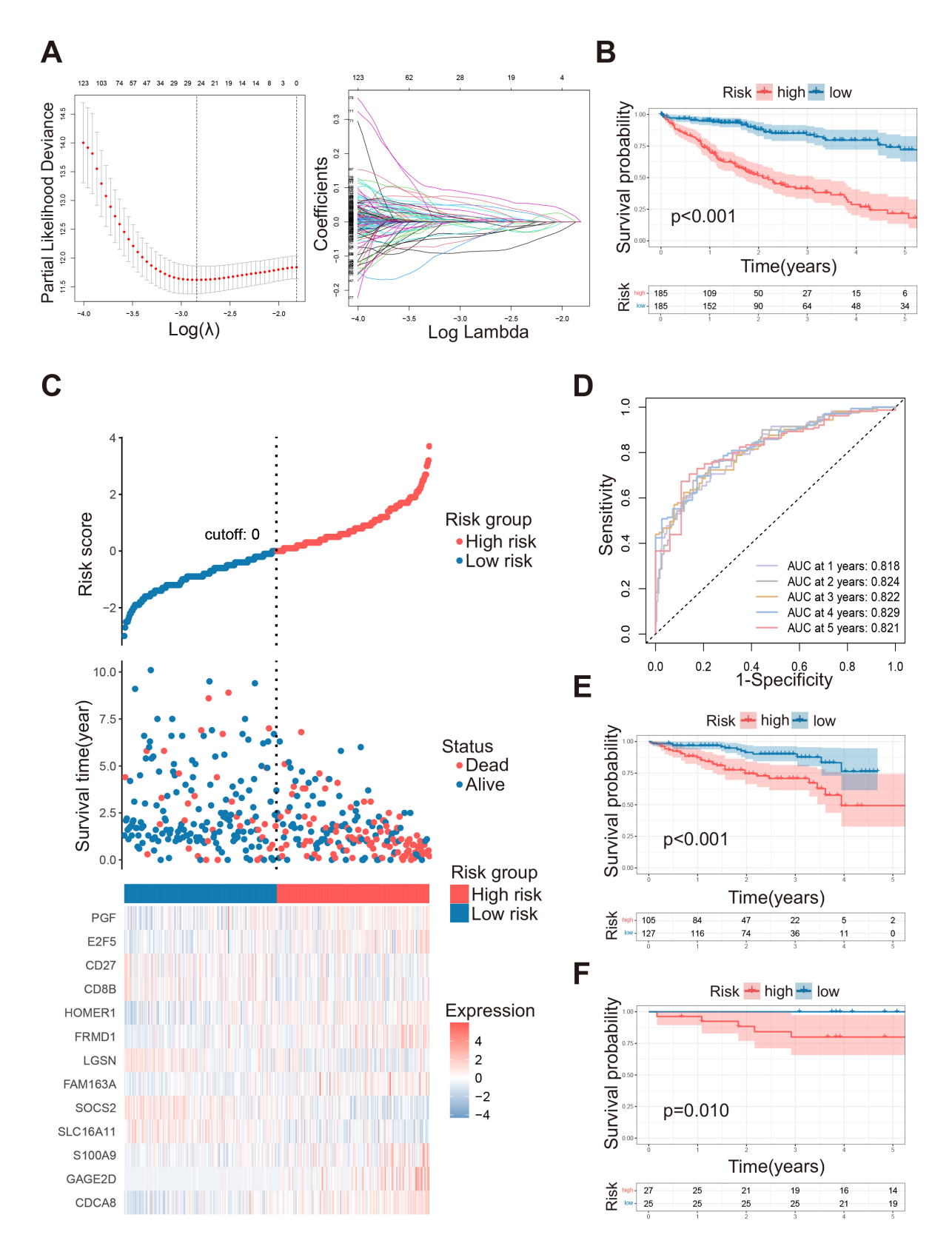
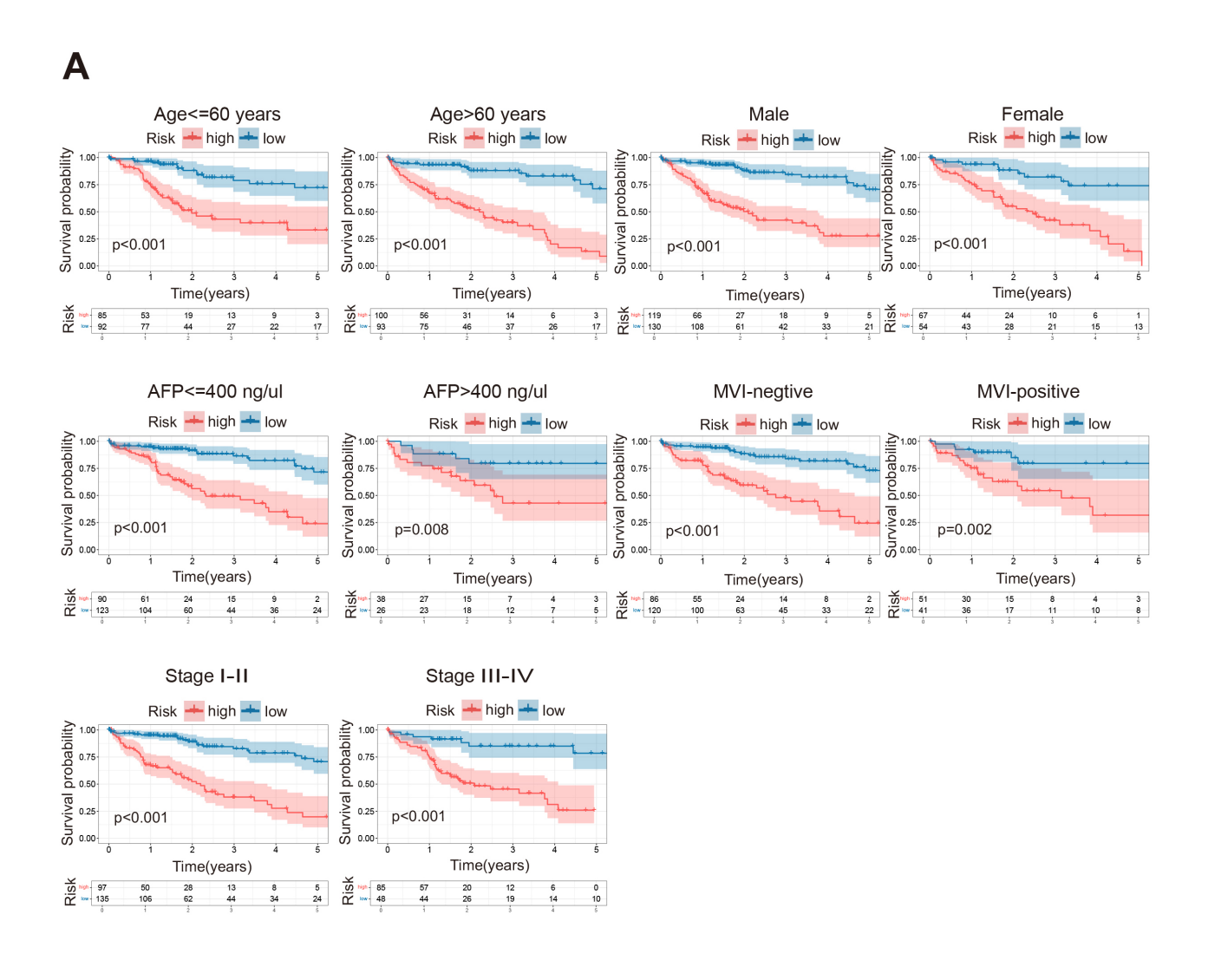


Fig. 4. Construction of HGL signature in LIHC. (A) Parameter selection for LASSO. (B) Kaplan-Meier survival curve analysis between high risk and low risk groups in TCGA-LIHC datasets. (C) Risk curves: overall survival status, and the heatmap of the expression of 13 HGL signature associate genes. The dotted line represents the division of the median. (D) ROC curves of the 1–5 years survival rates of TCGA-LIHC dataset. (E) Kaplan-Meier survival curve analysis between high risk and low risk groups in ICGC-LIHC datasets. (F) Kaplan-Meier survival curve analysis between high risk groups in GSE148355 datasets. LASSO, Least Absolute Shrinkage and Selection Operator; ROC, receiver operating characteristic.



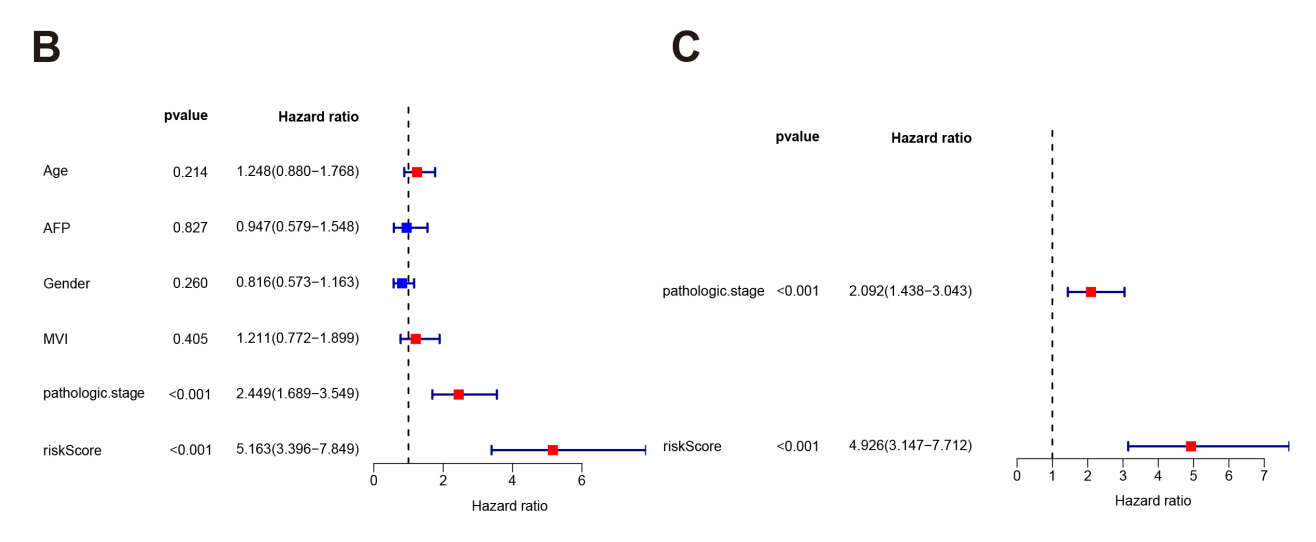


Fig. 5. HGL riskScore is an independent prognostic factor. (A) The Kaplan-Meier survival analysis was performed based on HGL risk signature for patients with different gender, with different ages, different AFP values, different MVI and pathological stages. (B) Forest plot showing Univariate-COX analysis of the TCGA-LIHC cohort including age, AFP, MVI, pathologic stage, and riskScore as variables. (C) Forest plot showing Multivariate-COX analysis including Pathologic stage, and riskScore as variables in the TCGA-LIHC cohort. AFP, alpha-fetoprotein level; MVI, microvascular invasion.



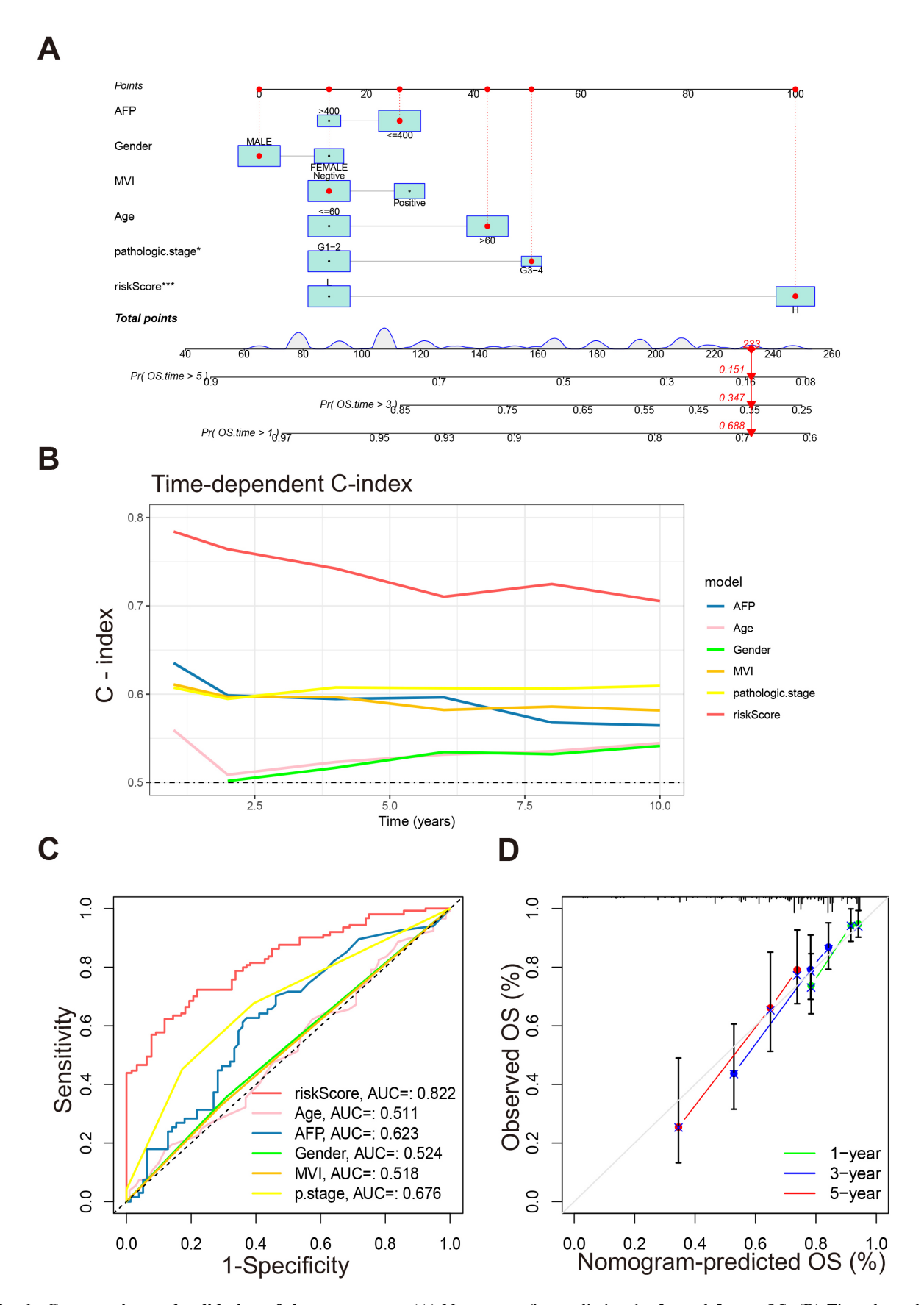


Fig. 6. Construction and validation of the nomogram. (A) Nomogram for predicting 1-, 3-, and 5-year OS. (B) Time-dependent C-index of riskScore and other clinical factors. (C) ROC curves of riskScore and other clinical factors predicting 3-year OS of patients. (D) Calibration curve for nomogram. *p < 0.05, ***p < 0.001. OS, Overall Survival.

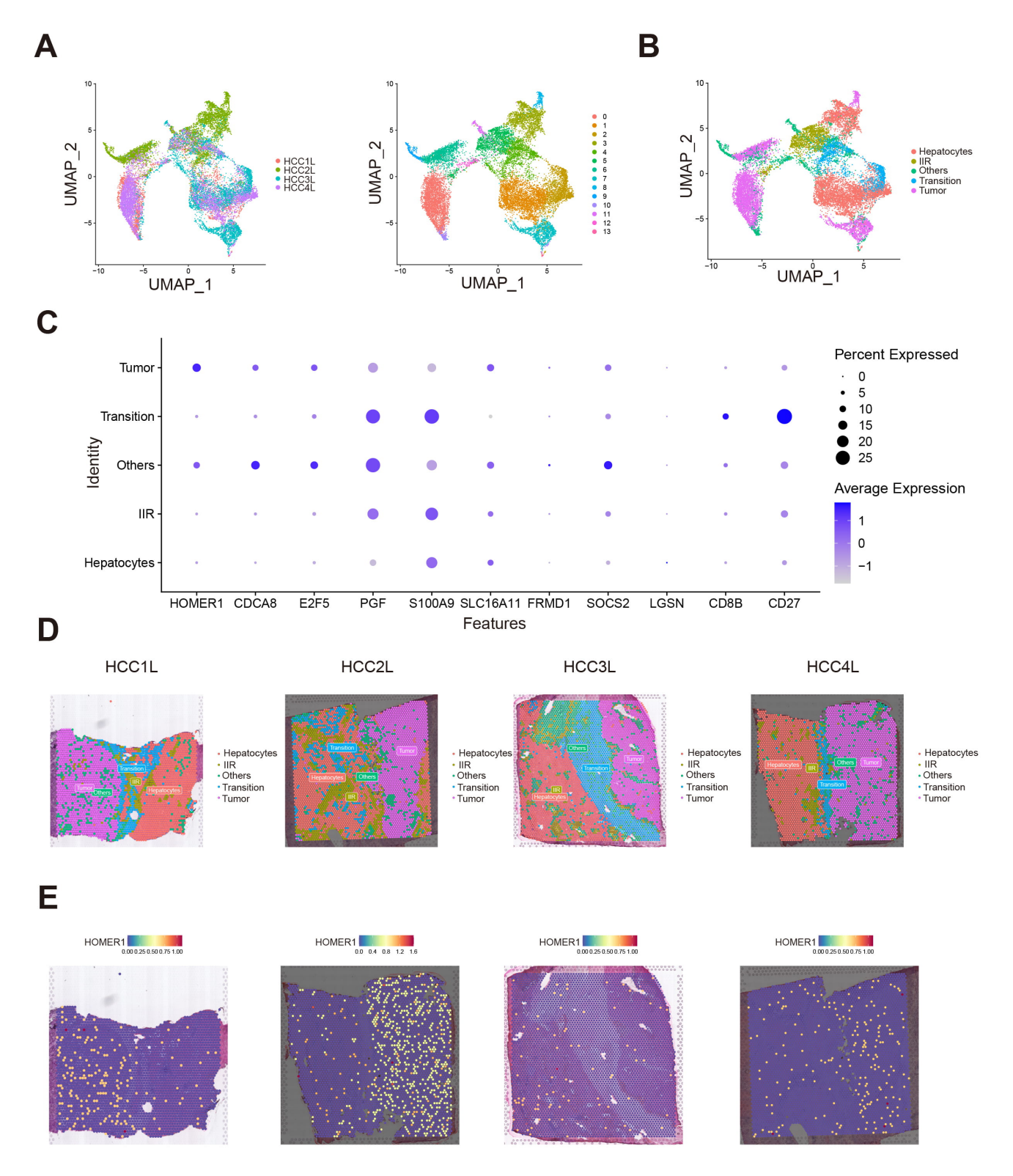


Fig. 7. Spatial transcriptome data revealing HOMER1 significantly enriched in hepatocellular carcinoma cell. (A) Four spatial transcriptome samples taken from the junction of hepatocellular carcinoma and para-carcinoma were analyzed by dimensionality reduction and cluster analysis, 14 different clusters were identified. (B) We identified clusters derived from Hepatocytes, Tumor, Immune infiltrate region (IIR), Transition, Others these five regions. (C) Bubble diagram showing genes expression in each region. (D) Spatial distribution of different cell clusters. (E) Spatial distribution of HOMER1 is concentrated in tumor cells. UMAP, uniform manifold approximation and projection.

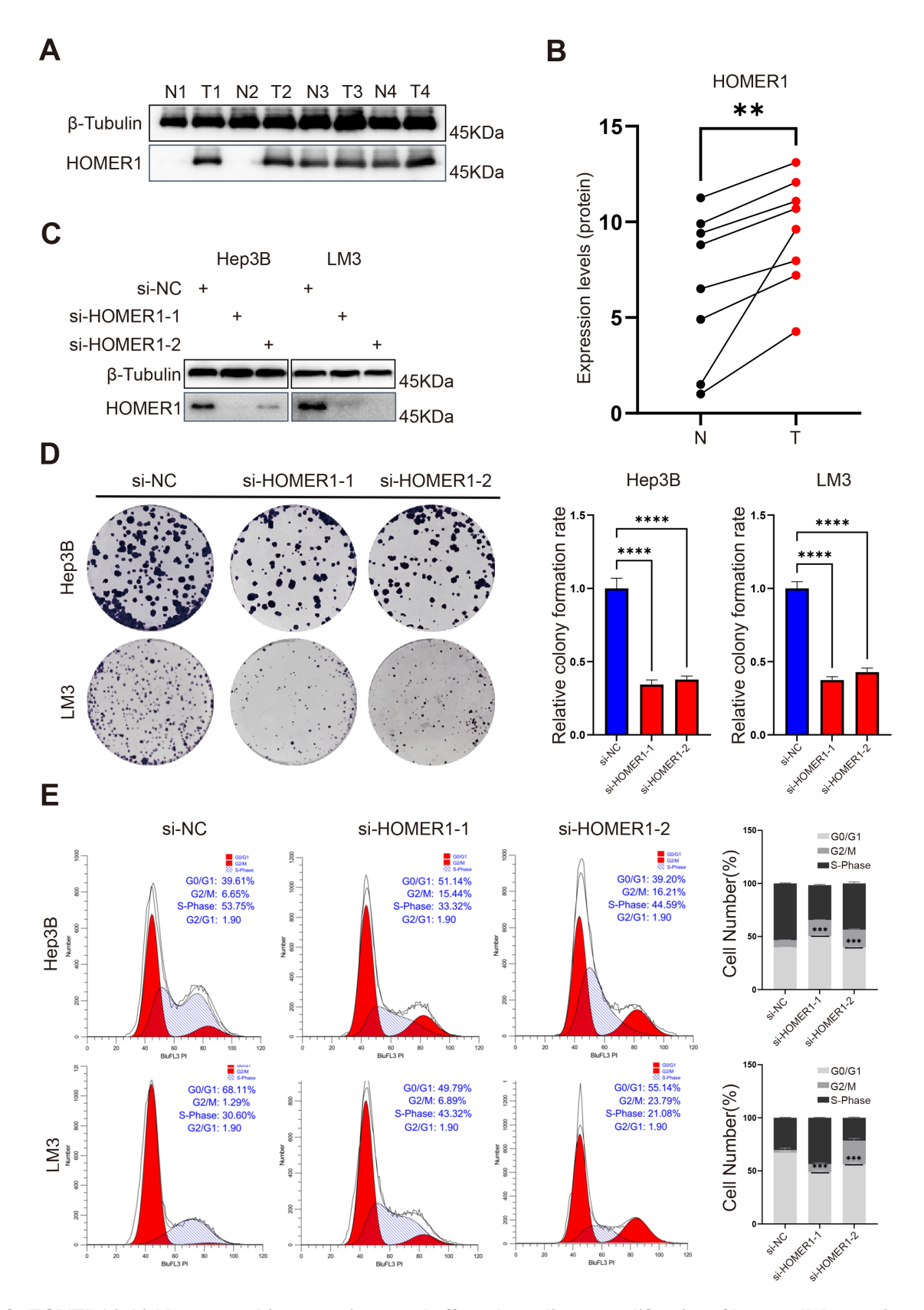


Fig. 8. HOMER1 is highly expressed in tumor tissues and affects the malignant proliferation of hepatocellular carcinoma cell lines. (A) Western Blot revealed that the expression of HOMER1 was evaluated in tumors and in adjacent tumors at the protein level. (B) The comparison of HOMER1 protein expression levels between normal and tumor tissues. (C) HOMER1 was successfully knocked down in LM3 and Hep3B cell lines. (D) The proliferation ability of LM3 and Hep3B decreased after knock down of HOMER1. (E) Knock down of HOMER1 blocked the cell cycle of LM3 and Hep3B. **p < 0.01, ****p < 0.001, ****p < 0.0001.

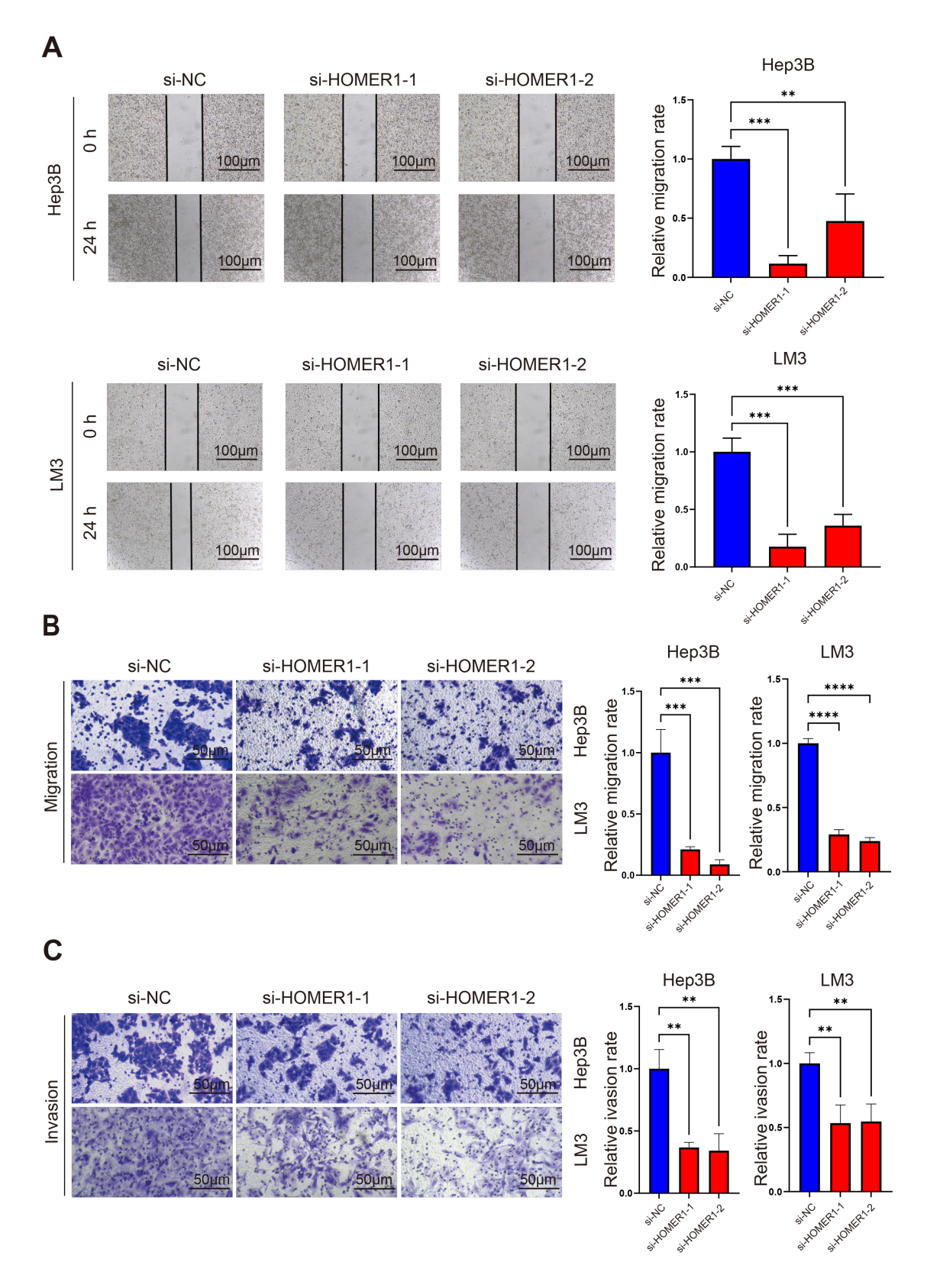


Fig. 9. The knocking down of HOMER1 affected the ability of metastasis and invasion of hepatocellular carcinoma cell lines. (A) The wound healing assay showed that knocking down of HOMER1 significantly decreased the migration ability of Hep3B and LM3. Scale bars = $100 \, \mu m$. (B) The Transwell migration assay showed that knocking down of HOMER1 decreased the migration ability of Hep3B and LM3. Scale bars = $50 \, \mu m$. (C) The Transwell invasion assay showed that knocking down of HOMER1 decreased the invasion ability of Hep3B and LM3. Scale bars = $50 \, \mu m$. **p < 0.01, ***p < 0.001, ****p < 0.0001.

veloped a 23-gene lactylation-related risk signature predicting the prognosis of colorectal cancer patients by the multi-dimensional approach; Cheng *et al.* [17] also constructed a 6-lactylation-related gene signature in gastric cancer; Cheng *et al.* [17] constructed an 8-gene signature using LASSO regression analysis in HCC, which revealed that lactylation-related signature can be used as biomarkers for effective clinical treatment of HCC. Several metabolites can act as substrates for histone modifications, while lactate is the product of glycolysis and also the substrate for lactylation. The hypoxic microenvironment in HCC promotes enhanced glycolysis, which may lead to lactate accumulation; and drives the transcription changes of genes related to the degree of histone modification and the malignant biological behavior of HCC.

In view of the crosstalk between metabolic reprogramming with lactylation, we co-included the hypoxiaglycolysis-lactate genesets in this study. Since lactylation plays a key role in a variety of cancers, we believe that such a signature will have great predictive significance for patients and also assistant in identifying genes associated with lactylation for further study.

We divided patients in TCGA-LIHC into two clusters based on the prognosis-associated HGL genes. There are significant differences in OS between the two clusters which reveals the HGL gene set is capable of increased stratification in patients with HCC, which also has implications for the use of drugs such as sorafenib, immune checkpoint inhibitors, and others. In order to independently predict the prognosis of each patient, we performed LASSO COX regression analysis on the differential expressed genes between clusters and obtained a 13-gene HGL signature (CDCA8, GAGE2D, S100A9, SLC16A11, SOCS2, FAM163A, LGSN, FRMD1, HOMER1, CD8B, CD27, E2F5, PGF). The signature has good prediction accuracy in the TCGA-LIHC training set, also in the test set ICGC-LIHC with a slightly smaller number of patients, in the external validation set GSE148355. Due to the small number of patients in this dataset, the AUC at the first year is not satisfactory, but still shows some prognosis for the long-term survival of patients. In terms of prediction accuracy and specificity, this signature is superior to previously reported hypoxia-related signatures [26], glycolysis-related signatures [12,27], and lactylation-related signatures [17]. It is also an independent prognostic factor for HCC patients.

The spatial transcriptome data revealed that, among the 13 genes, *HOMER1* was mostly expressed in tumor cells and was concentrated most in tumor regions, suggesting that *HOMER1* may have a critical role in the progression of hepatocellular carcinoma. It has been reported that circ-HOMER1 could regulate the growth and aggressiveness of hepatocellular carcinoma cells [28]. However, circ-HOMER1, as a circular RNA, is structurally and functionally different from the protein-coding *HOMER1* gene. Although HOMER1 has been reported to be associated with tumor biology and also has potential clinical application in

Hepatitis B Virus (HBV)-related HCC [29], there is still a lack of experimental verification for its mechanism. To investigate the effect of HOMER1 on HCC, we knocked it down in two cell lines, LM3 and Hep3B. We observed that knocking down of HOMER1 significantly inhibited cell proliferation which was confirmed by colony formation assays, while cell cycle analysis suggested that knocking down of HOMER1 effectively blocked the cell cycle. Wound healing assay and Transwell assay showed that knocking down of HOMER1 also inhibited the migration and invasion of LM3 and Hep3B. It is a novel discovery that HOMER1 affect the growth and invasiveness of HCC by blocking the cell cycle, which also reveals the possibility of HOMER1 as a potential therapeutic target for HCC.

However, this study still has some limitations. First, it does not provide specific guidance for the treatment of HCC patients. Second, we only investigated the effect of HOMER1 on the malignant progression of HCC, but didn't explore its mechanism, nor did we explore the relationship between HOMER1 and lactylation.

5. Conclusion

In this study, we constructed an HGL prognosisrelated signature to predict the prognosis of HCC patients, which has great predictive effect for patients in multiple data sets. We also found that HOMER1 can block the cell cycle and malignant progression of hepatocellular carcinoma, suggesting its potential as a new therapeutic target for hepatocellular carcinoma.

Availability of Data and Materials

The datasets analyzed in this study are available in the Cancer Genome Atlas (TCGA) database (https://www.cancer.gov/ccg/research/genome-sequencing/tcga), Gene Expression Omnibus (GEO) database (https://www.ncbi.nlm.nih.gov/geo/) and the International Cancer Genome Consortium (ICGC) database (https://platform.icgc-argo.org/). The datasets used and/or analyzed during the current study are available from the corresponding author on reasonable request.

Author Contributions

Conceptualization: KF; Data curation and Investigation: FY, SL, YY; Supervision: KF. All authors contributed to editorial changes in the manuscript. All authors read and approved the final manuscript. All authors have participated sufficiently in the work and agreed to be accountable for all aspects of the work.

Ethics Approval and Consent to Participate

The study was carried out in accordance with the guidelines of the Declaration of Helsinki. The study involving human patients were reviewed and approved by the Central South University Xiangya Hospital Research Ethics Committee, Ethics Number 202004191. Patients or their



families/legal guardians provided their written consent to participate in the study.

Acknowledgment

The authors appreciate the tutors who conducted the experiment and corrected the paper, the TCGA, ICGC, GEO dataset who provided the data sources for this article, and finally the patients who provided the organization. Finally, we would like to thank Professor Wen-Zheng Li for providing ethical approval support for this study.

Funding

This work was supported by National Natural Science Foundation of China [32170726] to KF.

Conflict of Interest

The authors declare no conflict of interest.

Supplementary Material

Supplementary material associated with this article can be found, in the online version, at https://doi.org/10.31083/FBL33422.

References

- [1] Tang H, Cao Y, Jian Y, Li X, Li J, Zhang W, et al. Conversion therapy with an immune checkpoint inhibitor and an antiangiogenic drug for advanced hepatocellular carcinoma: A review. Bioscience Trends. 2022; 16: 130–141. https://doi.org/10.5582/bst.2022.01019.
- [2] Vogel A, Meyer T, Sapisochin G, Salem R, Saborowski A. Hepatocellular carcinoma. Lancet. 2022; 400: 1345–1362. https: //doi.org/10.1016/S0140-6736(22)01200-4.
- [3] Llovet JM, Zucman-Rossi J, Pikarsky E, Sangro B, Schwartz M, Sherman M, et al. Hepatocellular carcinoma. Nature Reviews. Disease Primers. 2016; 2: 16018. https://doi.org/10.1038/nrdp.2016.18.
- [4] Rebouissou S, Nault JC. Advances in molecular classification and precision oncology in hepatocellular carcinoma. Journal of Hepatology. 2020; 72: 215–229. https://doi.org/10.1016/j.jhep .2019.08.017.
- [5] Yang X, Yang C, Zhang S, Geng H, Zhu AX, Bernards R, et al. Precision treatment in advanced hepatocellular carcinoma. Cancer Cell. 2024; 42: 180–197. https://doi.org/10.1016/j.ccell. 2024.01.007.
- [6] Faubert B, Solmonson A, DeBerardinis RJ. Metabolic reprogramming and cancer progression. Science. 2020; 368: eaaw5473. https://doi.org/10.1126/science.aaw5473.
- [7] Du D, Liu C, Qin M, Zhang X, Xi T, Yuan S, et al. Metabolic dysregulation and emerging therapeutical targets for hepatocellular carcinoma. Acta Pharmaceutica Sinica. B. 2022; 12: 558– 580. https://doi.org/10.1016/j.apsb.2021.09.019.
- [8] Jing X, Yang F, Shao C, Wei K, Xie M, Shen H, et al. Role of hypoxia in cancer therapy by regulating the tumor microenvironment. Molecular Cancer. 2019; 18: 157. https://doi.org/10. 1186/s12943-019-1089-9.
- [9] Infantino V, Santarsiero A, Convertini P, Todisco S, Iacobazzi V. Cancer Cell Metabolism in Hypoxia: Role of HIF-1 as Key Regulator and Therapeutic Target. International Journal of Molecular Sciences. 2021; 22: 5703. https://doi.org/10.3390/ijms22115703.

- [10] Wang S, Zhou L, Ji N, Sun C, Sun L, Sun J, et al. Targeting ACYP1-mediated glycolysis reverses lenvatinib resistance and restricts hepatocellular carcinoma progression. Drug Resistance Updates. 2023; 69: 100976. https://doi.org/10.1016/j.drup.2023.100976.
- [11] Wang F, Hu Y, Wang H, Hu P, Xiong H, Zeng Z, et al. LncRNA FTO-IT1 promotes glycolysis and progression of hepatocellular carcinoma through modulating FTO-mediated N6-methyladenosine modification on GLUT1 and PKM2. Journal of Experimental & Clinical Cancer Research. 2023; 42: 267. https://doi.org/10.1186/s13046-023-02847-2.
- [12] Chen D, Aierken A, Li H, Chen R, Ren L, Wang K. Identification of subclusters and prognostic genes based on glycolysis/gluconeogenesis in hepatocellular carcinoma. Frontiers in Immunology. 2023; 14: 1232390. https://doi.org/10.3389/fimmu.2023.1232390.
- [13] Feng J, Li J, Wu L, Yu Q, Ji J, Wu J, et al. Emerging roles and the regulation of aerobic glycolysis in hepatocellular carcinoma. Journal of Experimental & Clinical Cancer Research. 2020; 39: 126. https://doi.org/10.1186/s13046-020-01629-4.
- [14] Zong Z, Xie F, Wang S, Wu X, Zhang Z, Yang B, *et al.* AlanyltRNA synthetase, AARS1, is a lactate sensor and lactyltransferase that lactylates p53 and contributes to tumorigenesis. Cell. 2024; 187: 2375–2392.e33. https://doi.org/10.1016/j.cell.2024. 04.002.
- [15] Chen H, Li Y, Li H, Chen X, Fu H, Mao D, et al. NBS1 lactylation is required for efficient DNA repair and chemotherapy resistance. Nature. 2024; 631: 663–669. https://doi.org/10.1038/s41586-024-07620-9.
- [16] Yang Z, Yan C, Ma J, Peng P, Ren X, Cai S, et al. Lactylome analysis suggests lactylation-dependent mechanisms of metabolic adaptation in hepatocellular carcinoma. Nature Metabolism. 2023; 5: 61–79. https://doi.org/10.1038/ s42255-022-00710-w.
- [17] Cheng Z, Huang H, Li M, Liang X, Tan Y, Chen Y. Lactylation-Related Gene Signature Effectively Predicts Prognosis and Treatment Responsiveness in Hepatocellular Carcinoma. Pharmaceuticals. 2023; 16: 644. https://doi.org/10.3390/ ph16050644.
- [18] Li Q, Zhang J, Xiao S, Hu M, Cheng J, Yao C, et al. The impact of liver fibrosis on the progression of hepatocellular carcinoma via a hypoxia-immune-integrated prognostic model. International Immunopharmacology. 2023; 125: 111136. https://doi.org/10.1016/j.intimp.2023.111136.
- [19] de Bartolomeis A, Barone A, Buonaguro EF, Tomasetti C, Vellucci L, Iasevoli F. The Homer1 family of proteins at the cross-road of dopamine-glutamate signaling. An emerging molecular "Lego" in the pathophysiology of psychiatric disorders. A systematic review and translational insight. Neuroscience and Biobehavioral Reviews. 2022; 136: 104596. https://doi.org/10.1016/j.neubiorev.2022.104596.
- [20] Schmidt MJ, Naghdloo A, Prabakar RK, Kamal M, Cadaneanu R, Garraway IP, et al. Polyploid cancer cells reveal signatures of chemotherapy resistance. Oncogene. 2025; 44: 439–449. https://doi.org/10.1038/s41388-024-03212-z.
- [21] Dai X, Zhang N, Cheng Y, Yang T, Chen Y, Liu Z, et al. RNA-binding protein trinucleotide repeat-containing 6A regulates the formation of circular RNA circ0006916, with important functions in lung cancer cells. Carcinogenesis. 2018; 39: 981–992. https://doi.org/10.1093/carcin/bgy061.
- [22] Wu R, Guo W, Qiu X, Wang S, Sui C, Lian Q, et al. Comprehensive analysis of spatial architecture in primary liver cancer. Science Advances. 2021; 7: eabg3750. https://doi.org/10.1126/sciadv.abg3750.
- [23] Charoentong P, Finotello F, Angelova M, Mayer C, Efremova M, Rieder D, et al. Pan-cancer Immunogenomic Analyses Reveal Genotype-Immunophenotype Relationships and Predictors



- of Response to Checkpoint Blockade. Cell Reports. 2017; 18: 248–262. https://doi.org/10.1016/j.celrep.2016.12.019.
- [24] Llovet JM, Castet F, Heikenwalder M, Maini MK, Mazzaferro V, Pinato DJ, *et al.* Immunotherapies for hepatocellular carcinoma. Nature Reviews. Clinical Oncology. 2022; 19: 151–172. https://doi.org/10.1038/s41571-021-00573-2.
- [25] Huang H, Chen K, Zhu Y, Hu Z, Wang Y, Chen J, *et al.* A multi-dimensional approach to unravel the intricacies of lactylation related signature for prognostic and therapeutic insight in colorectal cancer. Journal of Translational Medicine. 2024; 22: 211. https://doi.org/10.1186/s12967-024-04955-9.
- [26] Li K, Yang Y, Ma M, Lu S, Li J. Hypoxia-based classification and prognostic signature for clinical management of hepatocellular carcinoma. World Journal of Surgical Oncology. 2023; 21:

- 216. https://doi.org/10.1186/s12957-023-03090-x.
- [27] Kong J, Yu G, Si W, Li G, Chai J, Liu Y, *et al.* Identification of a glycolysis-related gene signature for predicting prognosis in patients with hepatocellular carcinoma. BMC Cancer. 2022; 22: 142. https://doi.org/10.1186/s12885-022-09209-9.
- [28] Zhao M, Dong G, Meng Q, Lin S, Li X. Circ-HOMER1 enhances the inhibition of miR-1322 on CXCL6 to regulate the growth and aggressiveness of hepatocellular carcinoma cells. Journal of Cellular Biochemistry. 2020; 121: 4440–4449. https://doi.org/10.1002/jcb.29672.
- [29] Luo P, Feng X, Jing W, Zhu M, Li N, Zhou H, et al. Clinical and Diagnostic Significance of Homer1 in hepatitis B virus-induced Hepatocellular Carcinoma. Journal of Cancer. 2018; 9: 683– 689. https://doi.org/10.7150/jca.22279.

